Flame interactions with acoustic and bulk mode instabilities in a pre-mixed dump combustor

D. B. Hann and J. A. Fitzpatrick

Department of Mechanical and Manufacturing Engineering
Trinity College, Dublin, Ireland
E-mail: hannd@tcd.ie.

Abstract

Measurements of convection velocity in a dump combustor are made from a sequence of heat release images and pressure and heat release measurements, taken at a higher sampling frequency, using a hybrid space-time cross-correlation technique. In this case the mean profiles of the images were correlated with the two types of time measurement and the phase of the resulting function was directly related to the convection velocity.

The measurements reported are for the case where no thermo-acoustic mode is stimulated so that the dominant modes are the Helmholtz and a shedding mode due to the interaction of vortex shedding with a partial acoustic mode. The shedding mode is shown to dominant at ϕ=0.68 but mode switching is shown to begin at ϕ=0.68.

The results for the convection velocity are shown in the Figure 1 and are consistent with the physical processes present in the combustor. From this it can be seen that the convection velocity at the dump plane initially decreases as the flow expands at the exit of the dump plane. At about X/D=1.5 the convection velocity increases as thermal expansion causes an increase in the velocity. The initial values at the dump plane are much higher than the isothermal flow rates due to buoyancy forces and the dilation of the flow.

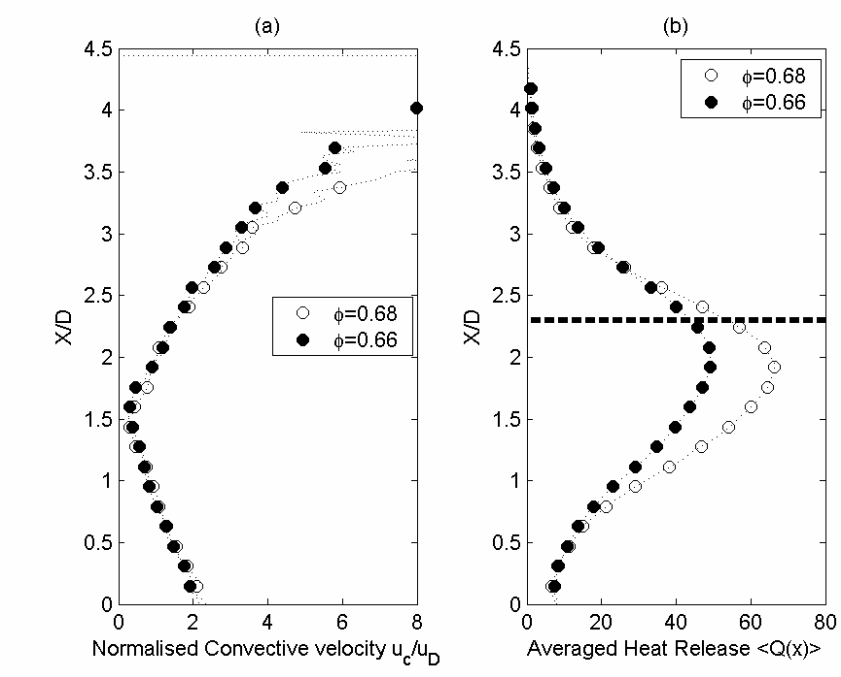

Figure 1: (a) Change in the measured convection velocity normalised by the isothermal dump plane velocity with downstream position and (b) mean heat release profiles.

Introduction

In recent years, there has been significant research to ensure more environmentally friendly combustion processes. One possible technique for reducing the emission of Nitrous Oxides and Carbon Monoxide is to make the combustion leaner. The main disadvantage to lean combustion is that significant instabilities may develop which can, in extreme circumstances, cause structural damage or blowout. Investigation of techniques to eliminate, or at least diminish these instabilities, by passive or active techniques are ongoing (e.g. Zaida and Graf 1998, Schadow et al 1987, Emeris et al 2003, Wang and Dowling 2003), but there is still some need to identify the physical mechanism occurring, since combustion is a hard environment in which to measure.

Much research has been done in the understanding and prediction of the thermo-acoustic modes where the acoustic mode feeds-back to generate fluctuations in the heat release (e. g. Dowling 1995, Langhorne 1988, Cho and Lee 1999, Bloxsidge et al 1988). Other possible mechanisms are a Bulk mode associated with the Helmholtz frequency and a shedding mode, where the shedding of vortex structures from the dump plane and the acoustic modes interact giving instabilities with higher frequencies than normal in the thermo-acoustic mode. The link between fluid dynamics and acoustics is more complicated and until recently a direct link between them remained to be determined (Gutmark et al (1991)).

A ray tracing theory was developed by Hann and Fitzpatrick (2004a) to predict the frequency excited when shedding motions stimulate instability in the combustion rig. This rig was configured so that thermo-acoustic modes were not excited to allow the investigation of other mechanisms. The work has shown that there are two other possible types of instability present in the rig, a bulk mode associated with shedding at the Helmholtz frequency, and shedding modes generated by vortex structures created at the dump plane locking on to a partial acoustic (Hann and Fitzpatrick (2004a)).

Further work is needed to identify mechanisms which cause mode switching., when the dominant mode will change cyclically with a low frequency. Lieuwen et al (2001) and Hann and Fitzpatrick (2004a) have shown that the frequency of mode shifting was the same as the expected frequency caused by feedback between the pressure generated at the flame front and velocity fluctuations at the inlet that may cause equivalence ratio fluctuations. Lieuwen et al (2001) showed that even small velocity fluctuations could cause significant ϕ fluctuations. While the comparison of predictions and results is not conclusive it gives a possible mechanism for the effect of mode switching. Another possible mechanism for mode switching could be variation of the convective velocity due to dilation fluctuations. A change in the flame shape, such as a lengthening of the recirculation zone can change the buoyancy forces at the dump plane and the dilation of the fluid due to thermal expansion. If a feedback mechanism existed, this would be another possible cause of mode switching.

If the shape and position of the flame front are known, the instability frequencies can be predicted. These will be determined by the geometry of the dump combustor, the equivalence ratio of the gas (air/fuel ratio) and the speed of the flow. The experiments reported here were directed to investigate more fully the convection effects within the flame and to do this a hybrid space-time correlation function will be used.

Derivation of the Hybrid Space-time correlation function

The standard technique for determining the velocities of the fluid is to use a technique such as LDV or PIV which both need seeding. High-speed imaging will also allow the determination of convective velocities, but this is expensive. A technique is outlined here that allows the measurement of convective velocities from a combination of slow images and fast streaming data at a point. The technique is adapted from that used to identify convecting features from combined PIV and LDV data in Chatellier (2004) and is outlined in more detail in Hann and Fitzpatrick (2004b).

The space-time correlation coefficients between two quantities that are coincident can be approximated by

$$r_{12}(\partial x, t) \approx \frac{1}{N}\sum_{n=1}^{N} \frac{\overline{U_{1n}(\partial x, nDt)U_{2n}(\partial x, nDt + t)}}{s_{U1n}\, s_{U2n}} \qquad (1)$$

If the features of interest in the flow are predominantly convective, then the parameters at can be replaced by

$$U(x,t) = U(x + ct). \qquad (2)$$

This approximation can be used to show that

$$r(\partial x,t) \approx r(t) \otimes d\left(t - \frac{\partial x}{\overline{c(\partial x)}}\right) \quad (3)$$

where $\overline{c(\partial x)}$ is the average convective velocity between the coincident measurement point and ∂x, and $\otimes$ denotes a convolution.

In the Fourier plane, the normalized cross-spectral density will be simpler, and can be given as

$$C_{12}(\partial x,w) = FFT\left\{ r_{12}(t) \otimes d\left(t - \frac{\partial c}{\overline{c(\partial x)}} \right) \right\} = C_{12}(w).e^{iw\,\partial x / \overline{c(\partial x)}}. \quad (4)$$

Therefore any coherent peak in the Fourier plane will have a magnitude related to the correlation coefficients, and a phase that is the sum of the difference in phase between the two signals at the coincident point and the phase due to convection of the features to and from the coincident position. As long as the correlation coefficient is greater than a threshold level, accurate predictions of the convection velocity can be made without the need for velocity measurements, or a high-speed camera.

Experimental procedure

The experiments presented were performed in a custom-made laboratory combustor rig with the dimensions as given in Table 1, and as shown in Figure 2. Air and fuel are combined as they enter the pre-mixer and the swirling flow generated by the tangential entrance fully mixes the gas before it emerges as a confined jet at the dump plane. Two equivalence ratios are presented here ϕ=0.68 and 0.66, corresponding to two different gas flow rates. The airflow rate can be approximated as constant between the two flows since the change in the flow rate is less than 1%. The flow has a Reynolds number of 17150 based on the isothermal flow through the dump plane and so can be considered fully turbulent. The two gas flow rates shown here correspond to 9.8KW and 9.5 kW. The combustion was analysed by the measurement of the spatial distribution of the heat release by imaging, by the temporal measurement of the heat release at a point at a much higher sample frequency, and the measurement of the wall pressure in the flame zone.

The images were captured by the use of a PCO Sensicam and the LAVision software. The 'super pixel' binning procedure was used to increase the signal to noise ratio of the faint flame images, and to allow capture at a rate of 23 Hz. The binning had to be set to 8 x 8 to allow good imaging of the flame with a 0.5 ms exposure time. Synchronisation of the images to the other data was maintained by the simultaneous recording of the triggering pulse for later comparison. To make the images relevant, a narrowband filter of 430 $\pm$ 10 nm was used to allow detection of the chemiluminescence of the OH radicals. The brightness of this wavelength gives an image where the intensity is directly proportional to the heat release (Hurle et al 1968).

The heat release was also measured by the use of a similarly narrowband filtered photomultiplier, which was focused along the main axis in the flame zone at a point coincident in height with the water cooled transducer used for the pressure measurements at 0.046 m from the dump plane. The triggering pulse, the pressure readings and the heat release data were captured at a rate of 6250 kHz simultaneously so there was no phase lag between them.

Table 1: Main parameters for the experiment.

Parameter	notation	value/range
Upstream Length	L_u	0.2 m
Downstream length	L_d	0.64 m
Nozzle diameter	D	0.02 m
Width of tube	2d	0.07 m
Volume rate of gas (lpm)	V_{gas}	16.8,17.3
Volume flow rate of Air (lpm)	V_{air}	242 lpm
Dump plane area expansion ratio	E_r	01:18

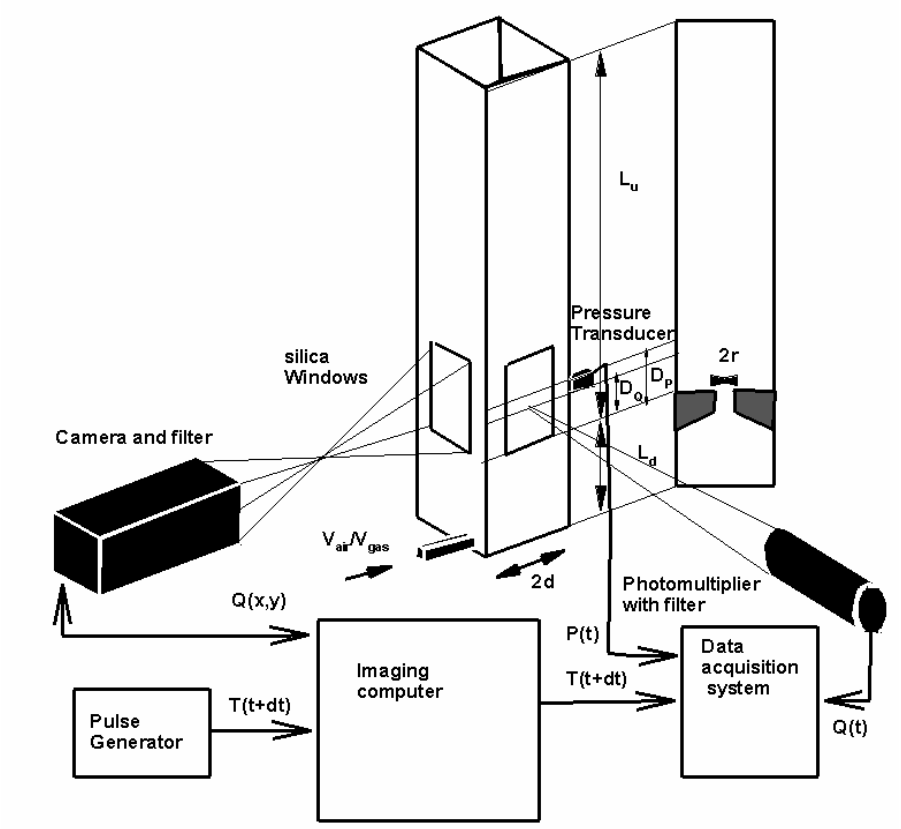

Figure 2: Schematic diagram showing the relationships between the various measurement techniques.

Results

The decrease in the total heat release as the equivalence ratio becomes leaner will change the stability of any resonance formed. Figure 3 shows how the averaged values in the image of heat release decreases as this happens. This decrease in maximum intensity is also related to the spread of the heat release over a larger area. This spread can be seen in Figure 4, which also shows that the position of maximum burning also moves downstream as the equivalence ratio increases.

At particular equivalence ratios, the system becomes unstable and mode switching occurs as can be seen in Figure 5. The parameters of the tube determine that the thermo-acoustic mode will not be stimulated, so the main frequency is the second order shedding mode frequency as defined by Hann and Fitzpatrick (2004a). Vortex driven instabilities have been shown by Gutmark and Ho (1983) and Gutmark et al (1991) to be most stimulated when the Strouhal number is between $0.2 < St < 0.5$. The Strouhal number in this experiment is in the region of St=0.35 based on the isothermal flow through the dump plane. The Shedding mode frequency is constant for ϕ=0.68 at 256 Hz, but as the energy of the flame is spread over a larger area at ϕ=0.66, that frequency becomes intermittent with the frequency locking on to the Helmholtz frequency at 213 Hz, before the instability dies out, only to be reactivated again at the shedding frequency.

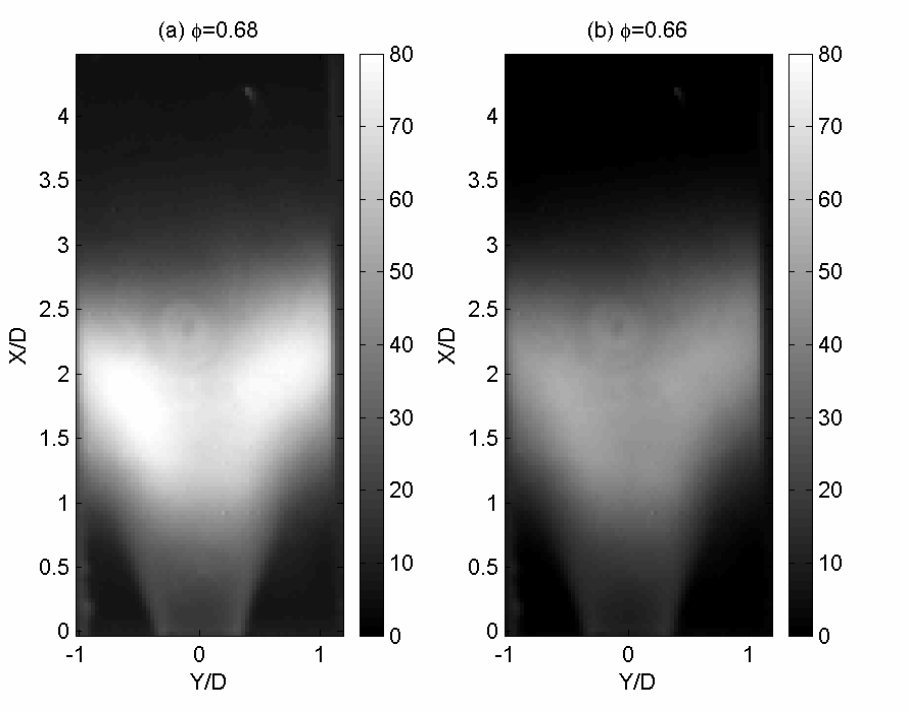

Figure 3: Average images of the heat release for the two equivalence ratios.

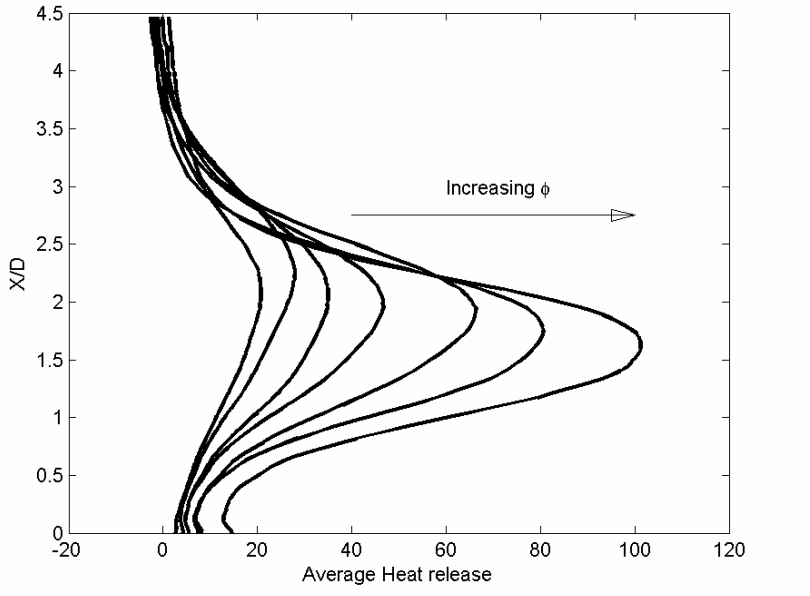

Figure 4: Variation in the averaged profile with decreasing equivalence ratio.

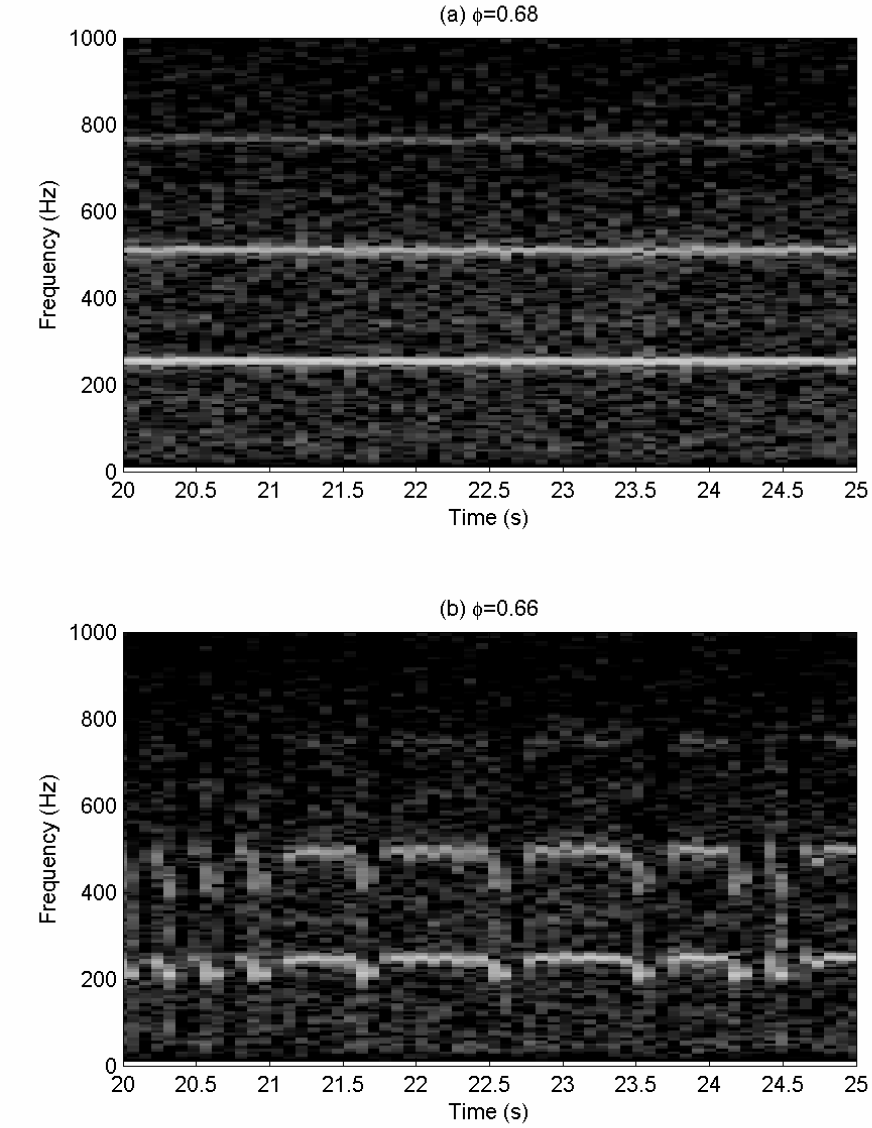

Figure 5: The Time-Frequency diagrams of segments of the heat release signal for the two equivalence ratios showing mode switching at f=0.66.

It can also be seen that harmonics of both frequencies exist, but this is most probably due to amplitude modulation effects as the heat release region will not be sinusoidal in magnitude as they pass through the measurement point.

The significant peaks in the auto-spectra of the pressure and heat release (Figure 6a and b) at ϕ=0.66 are the shedding mode peak at 256 Hz and the acoustic mode of the entire length of the combustor which has a peak at 760 Hz. The frequencies of these peaks decrease (244 Hz and 740 Hz) as the drop in ϕ causes a decrease in the downstream temperature. The acoustic mode peak is only present in the pressure measurements, which is consistent with predictions from Dowling (1995) that suggest that there is no feedback between the pressure and heat release at the acoustic frequency for this geometry and flow rate.

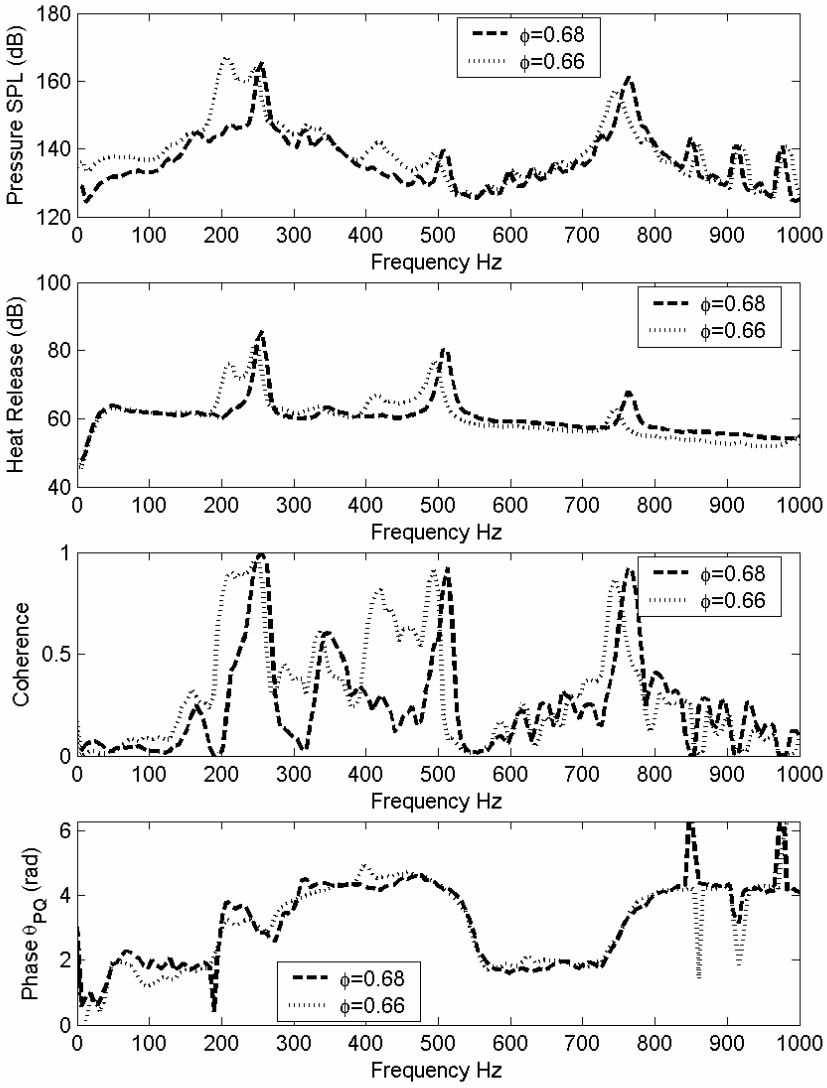

Figure 6: Spectral analysis of time signals. (a) Auto-spectrum of the pressure, (b) Auto-spectrum of the heat release, (c) coherence between the pressure and heat release and (d) phase between the pressure and the heat release.

There is strong coherence between the pressure and heat release at the shedding mode frequency for both equivalence ratio values and the Helmholtz frequency for ϕ=0.68. There is also a relatively strong coherence at the frequency of ~360 Hz, which corresponds to the 3rd order shedding mode which has been shown by Hann and Fitzpatrick (2004a) to be related by equation (5).

$$f = \frac{(n+0.25)}{t} \tag{5}$$

Where n is the order of the mode stimulated and τ is the time of propagation of the disturbance to return to the dump plane after travelling the full length of the combustor. This time consists of convective terms as well as propagating terms since the time of convection of the velocity disturbance to the flame front is the

largest component of τ. The phase between the pressure and heat release at the shedding mode changes from $\theta = 0.90\pi$ to π as ϕ decreases.

Hybrid Space-Time correlation results

Figure 7 shows the form of the hybrid ST-correlation functions between the instantaneous mean profile of each image and the pressure and heat release and it can be seen that both have similar forms. The correlation function at X/D=2.3 will in fact be an approximation for the cross-correlation function between the pressure and heat release. Because of the multi-frequency nature of this function it is more informative to analyse this function in the Fourier plane.

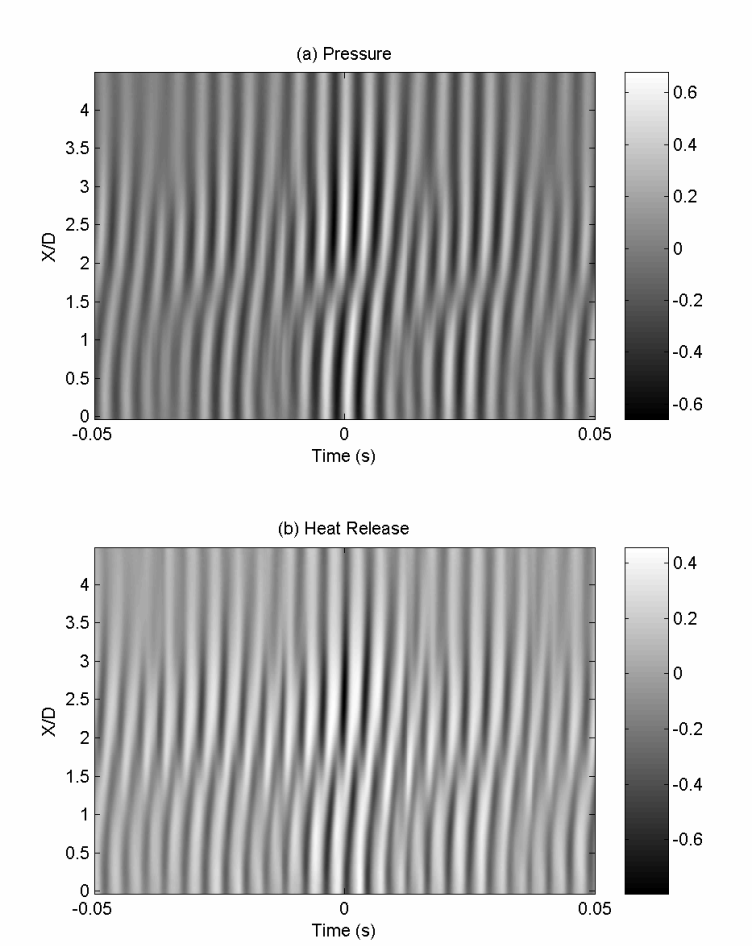

Figure 7: Hybrid ST-Correlation results for f=0.66 between the instantaneous mean profile of the heat release images and (a) the pressure and (b) the heat release.

The Fourier plane is shown in Figure 8, and the peaks can be seen to be similar to those in the auto-spectra. The magnitude and phase of the significant peaks will give information about the convective velocity as discussed earlier and these are shown in Figure 9. The phase (θ) between the heat release data and the heat release images is zero at the coincident point, and the phase between the pressure data and heat release data is $\theta = -0.9\ \pi$ (ϕ=0.66) and $\theta = -\pi$ (ϕ=0.66) which corresponds to the negative of the phase between the pressure and heat release data. The phase changes as the correlation moves away from the coincident points between the data, corresponding to a change in the convection of the data. The correlation coefficients are highest where the data is coincident and where the heat release was most significant which is why the coefficient falls to below 0.1 at positions further than the extent of the flame (X/D >0.35).

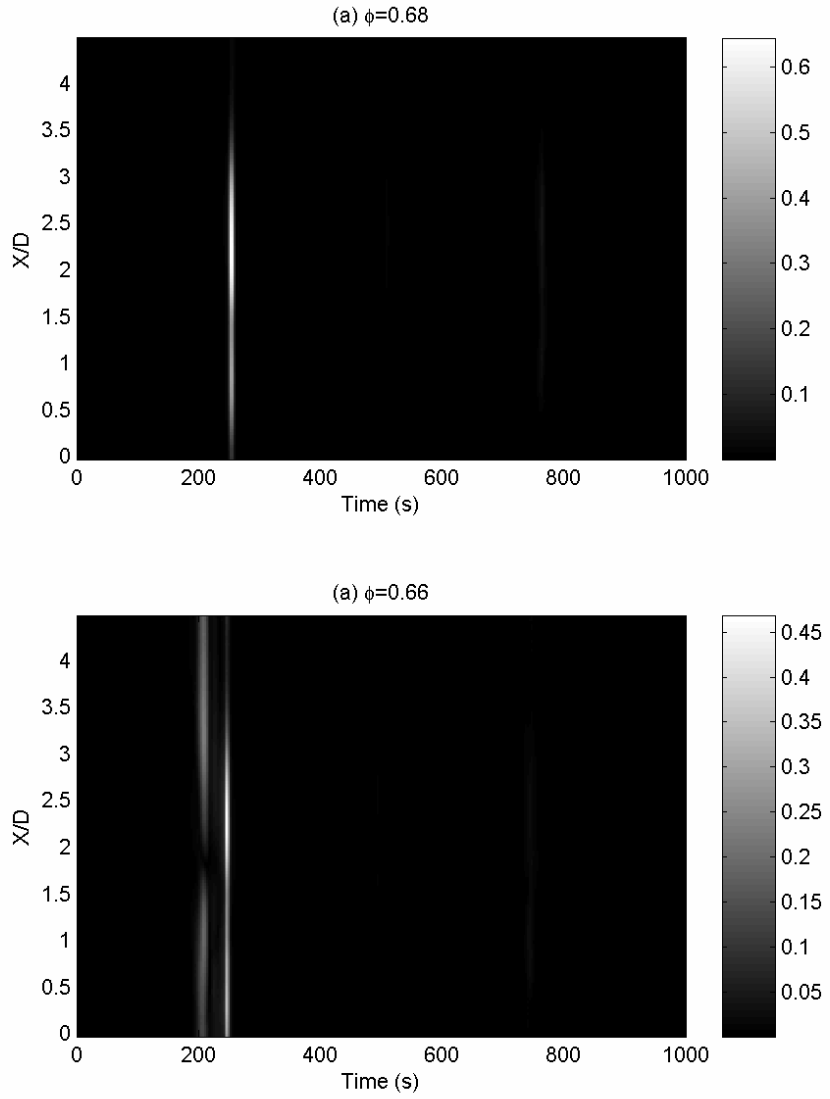

Figure 8: Hybrid ST Cross-spectral function for (a) f=0.68 and (b) f=0.66. Magnitude is linear value of the correlation coefficients.

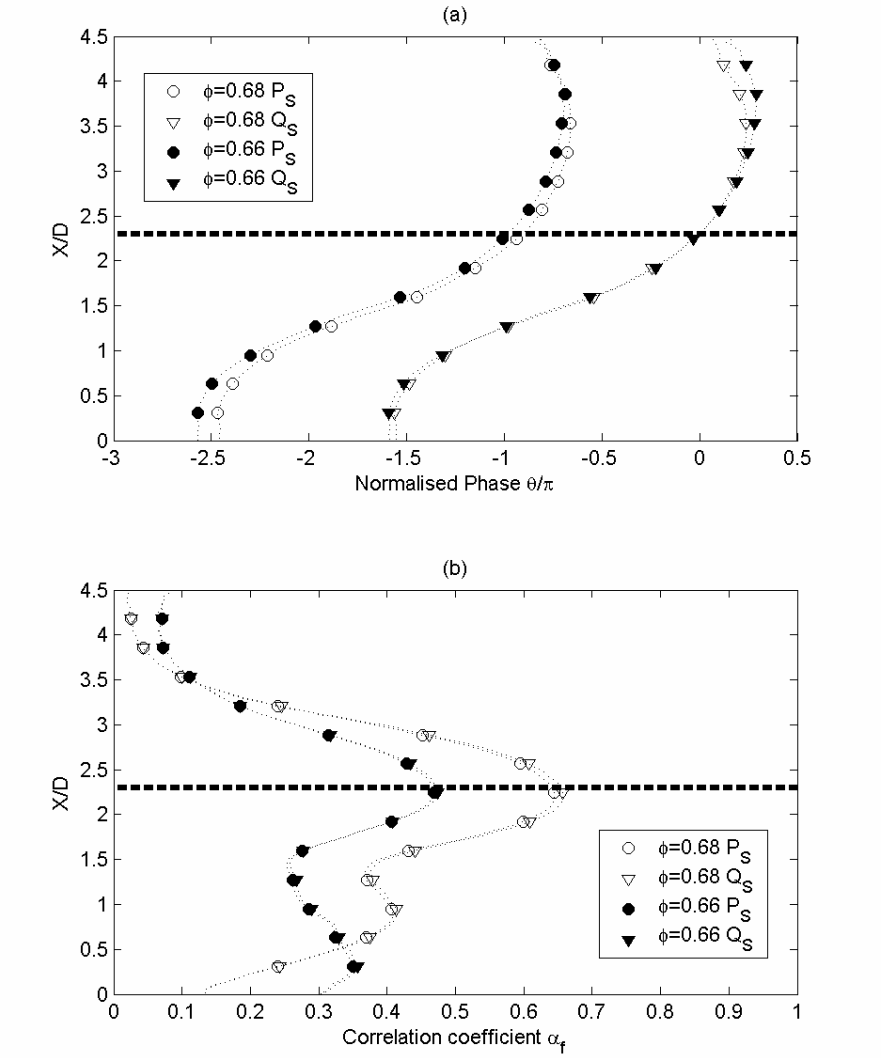

Figure 9: (a) the phase of the shedding peaks from the heat release data (Q_s) and the pressure data (P_s) and the (b) the correlation coefficient associated with that frequency.

The convection velocity can be easily calculated from the phase shown in Figure 9a and is shown in Figure 10a. The form of the convective velocity derived using this technique makes physical sense. The velocity decreases as the flow expands, and then accelerates as the flame causes an increase of the temperature in accordance with the distribution of heat release shown in Figure 10b. The rate of increase is dependent on the equivalence ratio with the acceleration being faster for ϕ=0.68. Quantitatively the increase in the convection velocity close to the dump plane is of the order two, possibly due to dilation as suggested by Milosavljevic et al (1990).

The convection velocity changes by 10% at the dump plane as the equivalence ratio is decreased, consistent with the decrease in the dilation due to a lower downstream temperature. The correlation coefficients fall below 0.1 above X/D=3.5 and the measurement becomes more noisy and unreliable.

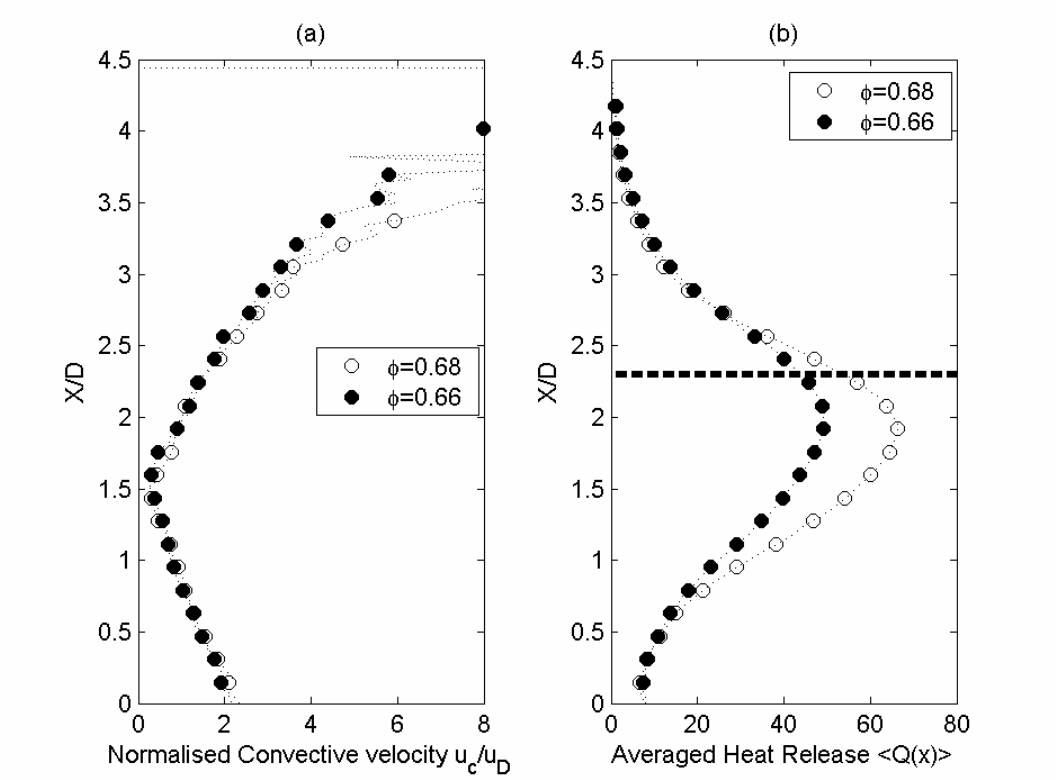

Figure 10: (a) Change in the measured convection velocity normalised by the isothermal dump plane velocity with downstream position and (b) mean heat release profiles.

Conclusion

Images of heat release and time-resolved measurement of the heat release and pressure have been combined to obtain information of features in the flow. The hybrid space-time correlation function can give the phase between time-resolved pressure data and images of heat release at the coincident point, and can be analysed at points away from the common point to obtain the convection velocity. These convection velocity measurements are consistent with understanding of the physical effects present in the flow, but it will be necessary to compare them directly with direct velocity measurements to confirm the validity of the analysis.

It is expected that there will be a critical threshold correlation coefficient related to the number of images and the standard deviations of the two signals above which the results will be valid. The technique can be used to investigate interaction of the shedding motions convected by the fluid in the combustor with the acoustics, since the position of the flame front is related to the dilated convection velocity, not the isothermal convection velocity.

Acknowledgements

The authors would like to acknowledge the support of the Marie Curie Host Development Fellowship programme of the European Commission under contract No. HPMD-CT-2000-00022.

References

Bloxsidge, G. J., Dowling, A. P., and Langhorne, P. J., (1988), “Reheat buzz: an acoustically coupled combustion instability. Part 2. Theory”, Journal of Fluids Mechanics, vol 193, pp 445-473.

Chatellier, L., (2004), " Measurement and prediction of flow-structure interaction", Marie Curie Final Report, EU research program FP5, Contract No. HPMD CT-2000-00022.

Cheo, S. and Lee, S., (1999), "Characteristics of thermo-acoustic resonances in a ducted burner", Journal of the acoustic society of America", vol 105, pp 3584-3587.

Dowling, A. P., (1995), "The calculation of thermo-acoustic oscillations", *Journal of Sound and Vibration*, Vol: 180, pp 557-581.

Emeris, I., Korusoy, E, Sivasegram, S. and Whitelaw, J. H., (2003) Control of ducted flames by combinations of imposed oscillations and added fuel", International colloquium of Combustion and Noise control, Cranfield University.

Gutmark E. and Ho, C. M., (1983) "On the preferred modes and spreading rates of jets". *Physics of fluids*, 26 2932-2938.

Gutmark, E, Schadow, K. C., Sivasegaram, S., and Whitelaw, J. H., (1991) "Interaction between fluid-dynamic and acoustic instabilities in combusting flows within ducts". *Combustion science and technology* 161-166.

Hann, D. B. and J. A. Fitzpatrick, (2004a), "Identification of bulk and longitudinal instabilities in a laboratory pre-mixed dump combustor", Submitted to Journal of Sound and Vibration.

Hann, D. B. and J. A. Fitzpatrick, (2004b), "Comparison of temporal and spatial measurements of the heat release in a pre-mixed dump combustor", In preparation for Combustion and Flame.

Hurle, I. R., Price, R. B., Sugden, T. M. and Thomas A. (1968), "Sound emission from open turbulent premixed flames", Proceedings of the Royal Society of London A, vol 303, pp 409-427.

Lieuwen, T., Torres, H., Johnson C. and Zinn B. T. (2001). "A mechanism of combustion instability in lean premixed gas turbine combustors". *Journal of engineering for gas turbines and power* Vol: 123, pp 182-189.

Langhorne, P.J., (1988), "Reheat buzz: an acoustically couped combustion instability. Part 1 Experiment.", Journal of Fluid Mechanics, Vol 193, pp 417-443.

Milosavljevic, V. D., Sivasegaram, S. and Whitelaw, J. H., (1990), "Ve locity characteristics of oscillating ducted premixed flames", Experiments in Fluids, Vol 9, pp 111-115.

Schadow, K. C., Gutmark, E., Wilson, K. J., Parr, D. M., Mahan, V. A. and Ferrel, G. B., (1987), "Effect of shear flow dynamics in combustion processes", Combustion Science and Technology, Vol 54, pp 103-116.

Wang, C. H. and Dowling, A. P., (2003), "Actively tuned passive control of combustion instabilities", International colloquium of Combustion and Noise control, Cranfield University.

Zaida, S. and Graf, H., (1998), "Feedback control of combustion oscillations", Journal of fluids and structures", vol 12, pp 491-507.